

Cd and Te desorption from (001), (111)*B*, and (110) CdTe surfaces

S. Tatarenko

Laboratoire de Spectrométrie Physique, CNRS–Université Joseph Fourier, Boîte Postale 87, 38402 Saint Martin d' Heres Cedex, France

B. Daudin and D. Brun

Département de Recherche Fondamentale sur la Matière Condensée, Commissariat à l'Énergie Atomique, SPMM/LPI, 38054 Grenoble Cedex 9, France

V. H. Etgens

*European Synchrotron Radiation Facility (ESRF), Boîte Postale 220, 38043 Grenoble Cedex, France
and Laboratoire de Minéralogie-Cristallographie, 4 place Jussieu, 75005 Paris Cedex, France*

M. B. Veron

*Laboratoire pour l'Utilisation du Rayonnement Electromagnétique (LURE), Bâtiment 209D, 91405 Orsay, France
(Received 13 June 1994)*

The Cd and Te desorption from (001), (110), and (111)*B* CdTe surfaces have been studied as a function of temperature by measuring the electron beam current reflected from these surfaces. For Te, activation energies of 0.96, 1.23, and 2.04 ± 0.10 eV have been found for (001), (110), and (111)*B* surface orientation, respectively. For Cd, activation energies of 1.9 ± 0.1 and 1.96 ± 0.10 eV are measured for the (111)*B* and the (001) CdTe surfaces, respectively, similar to the measured values of activation energy for the sublimation of these surfaces. A detailed analysis of the desorption process gives some enlightenment concerning two remarkable phenomena, namely, (i) a reversible transformation between a $c(2 \times 2) + (2 \times 1)$ and a (2×1) reconstruction for (001) CdTe and (ii) a hysteresis cycle between a (1×1) and a $c(8 \times 4)$ surface for the (111)*B* CdTe.

I. INTRODUCTION

II-VI semiconductors are a subject of current interest for their potential applications as blue emitting devices and as infrared or x-ray detectors. In practice, the realization of such devices depends on the ability to grow high-quality material in reproducible conditions. In particular, the crystal quality of a layer grown by molecular-beam epitaxy depends on both the substrate temperature and on the II/VI flux ratio. As the surface structure also depends on these parameters, a correlation can be established between this structure and the bulk crystal quality. Hence, detailed knowledge of the surface stability is essential for controlling the growth process.

Some results concerning the activation energy for desorption of Cd and Te on (001) CdTe, on Cd-terminated (111)*A* CdTe, and on Te-terminated (111)*B* CdTe have been reported by previous authors.^{1–5} As the values obtained are rather scattered and sometimes contradictory with each other, it appeared useful to carry out detailed investigations on the stability of (001), (111)*B*, and (110) CdTe surfaces prepared in comparable experimental conditions.

The aim of this paper is to report Cd and Te desorption experiments performed on these three types of surfaces for temperatures ranging from 220 to 340 °C. The surfaces were prepared according to the procedure described in Sec. II and then saturated either with Cd or with Te. After suppression of the Te or Cd flux, the surface evolves to its under-vacuum stabilized state, some-

times through several intermediate stages, which can be correlated with characteristic surface reconstructions.

The main experimental technique was reflection high-energy electron diffraction (RHEED). The recovery time of the surface after stopping the extra flux was measured by recording the intensity variations of the specular spot. This technique is particularly well suited to the present study as structural surface transitions produce strong variations of the RHEED specular beam intensity, related to changes of surface stoichiometry.^{6,7} Some measurements have also been performed on the fractional-order streaks in the RHEED pattern. However, measurements of the intensity of a particular reconstruction line provide only partial information on the structural changes.

Measurements as a function of the substrate temperature T_s allowed us to determine the activation energies of the desorption of the atoms adsorbed during the exposure phase. In order to identify the bonding states of the desorbed species, we discuss the correlation of the desorption results with available informations about the surface reconstructions involved in the desorption process^{8,9} and with sublimation rate measurements.^{2–4,10}

II. SAMPLE PREPARATION AND TECHNICAL ARRANGEMENT

The samples used in this study were prepared in a conventional molecular-beam epitaxy apparatus equipped with CdTe, Te, and Cd effusion cells. The substrates were commercial CdZnTe wafers (4% Zn). After a stan-

dard cleaning procedure, they were chemically etched in a 0.5% bromine-methanol solution for 2 min. Then, they were fixed with gallium on a molybdenum sample holder and etched again for 30 s in a 0.25% bromine-methanol solution in order to remove the surface oxide. To prevent further oxidizing, the substrates were transferred into the introduction chamber under nitrogen atmosphere. In the growth chamber, the sample temperature was controlled by a thermocouple in contact with the rear face of the molybdenum sample holder, with an accuracy estimated to be $\pm 1^\circ\text{C}$.

Prior to the desorption measurements, a CdTe buffer layer was grown on the substrate in order to improve the crystal quality and to obtain a specular spot. Concerning the (001) and the (111)*B* surface orientations, growth was carried out according to the following procedure: (1) heating at 230°C for 20 min to desorb the amorphous Te layer deposited during the etching step; (2) growth of a CdTe buffer at 340°C for 10 min; followed by (3) a growth stage at 320°C . The best growth conditions were obtained with an excess Cd or Te flux for the (001) and (111)*B* orientations, respectively. For the (110) orientation, step 2 of the above procedure resulted in a severe degradation of the crystal. For this orientation, the best surface smoothing procedure was an annealing at 280°C under Te flux followed by a growth stage at 220°C for 30 s. This cycle was repeated several times, then a buffer could be grown at 220°C . The best growth was achieved with a strong Te excess, about five times the Cd flux.

The energy of the electron beam used for RHEED experiments was 34 keV and the angle corresponds to off-Bragg conditions. The RHEED pattern was monitored by a charge coupled device camera. The intensity of the specular beam or of a reconstruction line was measured using a photomultiplier coupled via an optical fiber to the video monitor. The desorption rates of Cd and Te were obtained by measuring the time taken to reach the stabilized RHEED intensity level, that is the level corresponding to the static surface under vacuum, after an exposure to Cd or Te fluxes. The pressures of Cd and Te were typically in the 5×10^{-7} Torr range.

III. (001) CdTe

A. Te desorption

When a (001) CdTe surface is exposed to a Te flux, a (2×1) surface reconstruction is observed in the whole temperature range of interest, namely $230\text{--}340^\circ\text{C}$. When the Te flux is stopped, several regimes are observed, depending on the substrate temperature. In the $230\text{--}285^\circ\text{C}$ temperature range, no change is seen in the surface reconstruction, which remains (2×1) , but an increase in the specular-beam intensity is measured as shown in Fig. 1(a). This indicates that the final (2×1) surface structure is distinct from the (2×1) surface under Te flux, in agreement with x-ray photoelectron spectroscopy (XPS) experiments, which have shown that the stoichiometry of a (2×1) surface stabilized under Te pressure at 230°C changes under vacuum above 250°C , due to Te desorption.⁹ The characteristic time necessary to reach the sta-

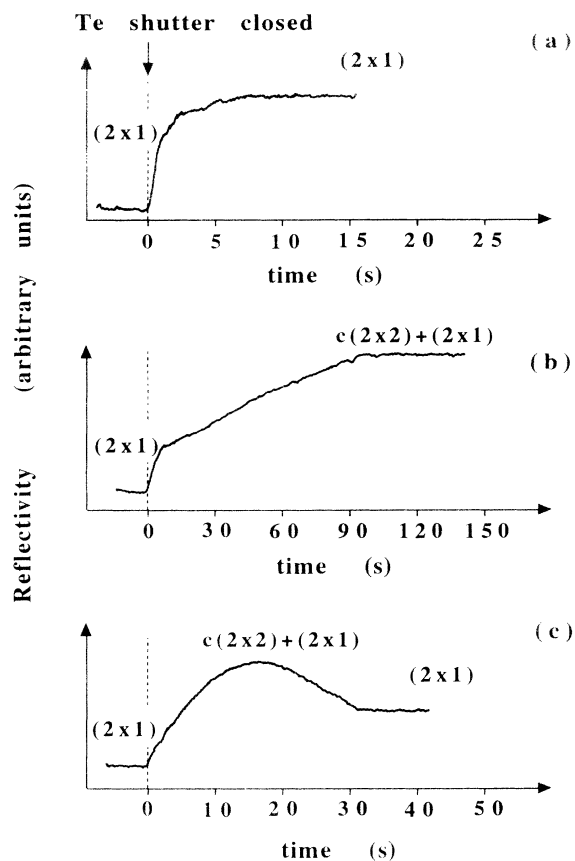


FIG. 1. Change of the RHEED specular-beam intensity as a function of time for (001) CdTe. (a) After stopping of the Te flux for $T_s = 255^\circ\text{C}$. (b) After stopping of the Te flux for $T_s = 292^\circ\text{C}$. (c) After stopping of the Te flux for $T_s = 339^\circ\text{C}$.

bilized surface state is plotted in Fig. 2 as a function of $1/T_s$, leading to the determination of an activation energy of 0.96 ± 0.10 eV for this process. This low value indicates that the Te atoms involved in the desorption process are weakly bound.

At higher temperature, above 285°C , a transition from

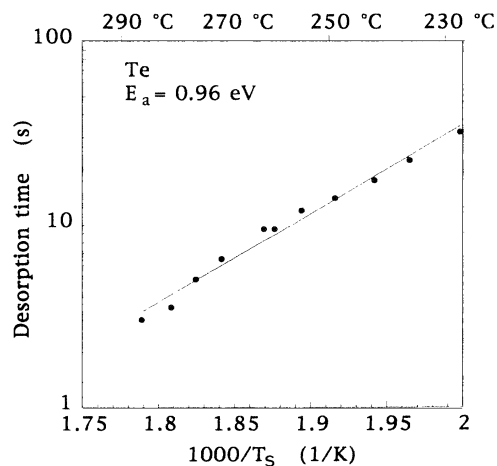


FIG. 2. Te desorption time deduced from measurements on (001) CdTe like those of Fig. 1 as a function of $1/T_s$, for T_s in the $225\text{--}285^\circ\text{C}$ range.

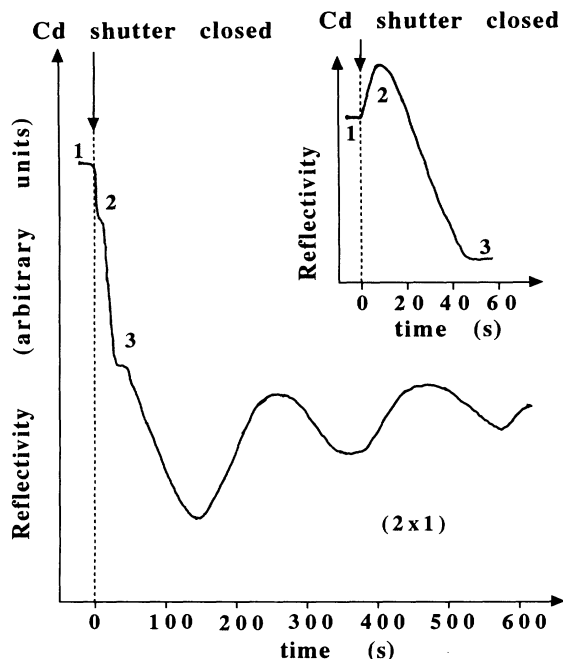


FIG. 3. Change of the RHEED specular-beam intensity for (001) CdTe, as a function of time, after shuttering of the Cd flux, for T_s above 300°C . The three stages identified before the onset of sublimation are marked 1, 2, and 3, the RHEED azimuth being $[110]$. Inset: Expansion of the initial stage recorded on RHEED azimuth $[100]$.

a (2×1) surface to a mixed $c(2 \times 2) + (2 \times 1)$ surface is observed. The evolution of the RHEED specular-beam intensity is shown in Fig. 1(b). From the measurement of the time necessary to form the $c(2 \times 2) + (2 \times 1)$ reconstruction as a function of the temperature, an activation energy of about 0.7 eV was found for this process. However, the activation energy determination was made difficult by the narrow temperature range involved. Actually, as shown in Fig. 1(c), above about 300°C the initial (2×1) surface evolves only in a first stage to a $c(2 \times 2) + (2 \times 1)$ one; this structure is not stable at high temperature and evolves to a (2×1) reconstruction and a plateau is finally observed. (Note that the transformation from a $c(2 \times 2)$ to a (2×1) structure is also observed during Cd desorption as will be discussed in the next section.) The plateau is followed by RHEED oscillations (see Fig. 3) indicating the sublimation of the CdTe in a layer-by-layer mode.

B. Cd desorption

When a (001) CdTe surface is exposed to a Cd flux, a $c(2 \times 2)$ surface reconstruction with a weak (2×1) contribution is observed in the whole temperature range explored, in agreement with previously published results.^{9,12} Up to 300°C no change of either the RHEED pattern or the RHEED specular-beam intensity is observed when the Cd shutter is closed. Above about 300°C , the surface reconstruction evolves to a (2×1) one in the absence of Cd flux. The evolution of the RHEED

specular-beam intensity at T above 300°C is shown in Fig. 3 in the $[110]$ azimuth for the main curve and in the $[100]$ azimuth for the inset. In a first step, a sharp variation of the intensity is observed. The shoulder (or the increase of the intensity for the inset) at the beginning of the desorption (step 2 in Fig. 3) corresponds to the complete disappearance of the weak (2×1) reconstruction observed under Cd flux (step 1 in Fig. 3) and, concomitantly, a reinforcement of the $c(2 \times 2)$ reconstruction. Then, a decrease associated with the formation of a (2×1) reconstruction is observed. A plateau (step 3 in Fig. 3) corresponding to the complete formation of this structure is brought out as shown in the inset of Fig. 3. Following the plateau, reverse RHEED oscillations occur (Fig. 3), which are characteristic of the sublimation of CdTe. It is worth pointing out that the maximum intensity of the oscillations corresponds to the intensity of the (2×1) plateau, which confirms that the sublimation process occurs in a layer-by-layer mode: a smooth (2×1) reconstructed surface being recovered after the sublimation of each monolayer. The kinetics of the sublimation process are detailed elsewhere.¹⁰

As concerns the $c(2 \times 2)$ to (2×1) transition, the desorption time necessary to reach the plateau corresponding to the above-mentioned step 3 is plotted in Fig. 4 as a function of $1/T_s$, leading to an activation energy of 1.96 ± 0.05 eV. According to the model proposed for the $c(2 \times 2)$ CdTe and ZnSe surfaces,^{10,13} which assume cation-terminated surfaces with a coverage of 50%, this energy should correspond to the desorption of Cd atoms bonded in two Te atoms. It is noteworthy that this value of activation energy is very close to the sublimation activation energy determined with reverse RHEED oscillations (1.90 eV).¹⁰

It is interesting to compare the previous results with recent grazing incidence x-ray diffraction (GIXD) experiments performed on (001) CdTe surfaces at the LURE synchrotron facility.¹¹ When a pure $c(2 \times 2)$ structure,

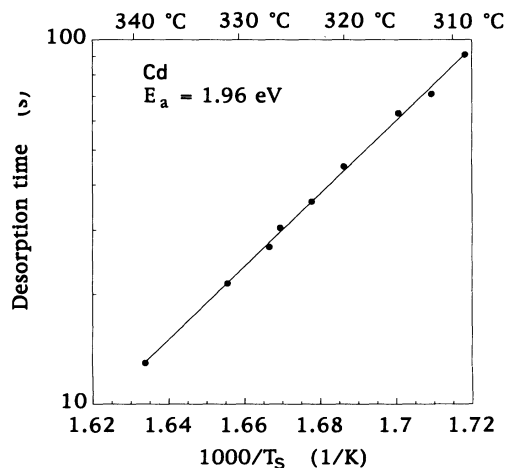


FIG. 4. Cd desorption time from (001) CdTe as a function of $1/T_s$, corresponding to the time for transition from the $c(2 \times 2)$ to the (2×1) surface reconstruction (time to reach step 3 in Fig. 3).

obtained by exposure of a (001) CdTe surface to a Cd flux at low temperature (about 200 °C), is heated under vacuum, one observes a continuous loss of the intensity of the peaks associated with the surface reconstruction. However, the half-width at half maximum of the peaks is constant during the heating process, which means that the size of the reconstruction domains remains unchanged. Above 310 °C, the $c(2 \times 2)$ surface disappears and a (2×1) reconstruction is observed. The GIXD experiments confirm the above interpretation of the RHEED evolution for a surface exposed to a Cd flux: no change of the surface structure below 300 °C and formation of a (2×1) surface above 300 °C.

In the same way, a (2×1) reconstruction associated with a Te-rich surface, obtained by exposing a CdTe surface to a Te flux at 220 °C, disappears above about 250 °C. A $c(2 \times 2)$ reconstruction appears around 290 °C before evolving about 310 °C to a (2×1) surface reconstruction, different from that observed at low temperature. The latter results are consistent with the RHEED observations reported above, which have demonstrated the desorption of Te from the (2×1) Te-rich surface at low temperature and the appearance of a $c(2 \times 2)$ surface at about 290 °C.

The occurrence of a reversible surface transformation in the 280–300 °C temperature range was also demonstrated by GIXD experiments.¹¹ As a matter of fact, if one starts from the (2×1) surface stabilized under vacuum at high temperature (320 °C), cooling down below 300 °C under vacuum results in the reappearance of the $c(2 \times 2)$ reconstruction, while the (2×1) is still present. Reheating up to 310 °C produces a disordering of the $c(2 \times 2)$ domains, while the (2×1) domains remain unchanged. A new cooling cycle induces the reappearance of the mixed $c(2 \times 2) + (2 \times 1)$ surface. GIXD experiments reveal that this mixed phase is formed by 50% of (2×1) and 50% of $c(2 \times 2)$ domains. This cycle is the experimental evidence for a reversible transformation under vacuum.

The above results on the reversible phase transformation favorably compare with XPS measurements,⁹ which have shown that a (001) CdTe surface initially stabilized with Te [(2×1) surface] or with Cd [$c(2 \times 2)$ surface] at low temperature eventually becomes Cd stabilized at 280 °C and that the Cd surface-atom desorption occurs above 300 °C, whereas cooling the sample below 300 °C leads back to a Cd stabilized surface.^{9,12,14} Moreover, it was demonstrated in the cited XPS study that each cycle of heating cooling through the reversible surface transformation temperature induces the desorption of half a monolayer of CdTe. The latter point is probably related to the existence of two equivalent domains in the mixed $c(2 \times 2) + (2 \times 1)$ surface.

The above observations concerning a reversible transformation under vacuum at 300 °C have been confirmed and completed in the present study by recording the variation of the RHEED intensity during the reversible transformation. The thermal cycle is illustrated in Fig. 5, which shows the variation of the RHEED specular-beam intensity, recorded as a function of the substrate temperature in the 280–305 °C temperature range. Initially, a

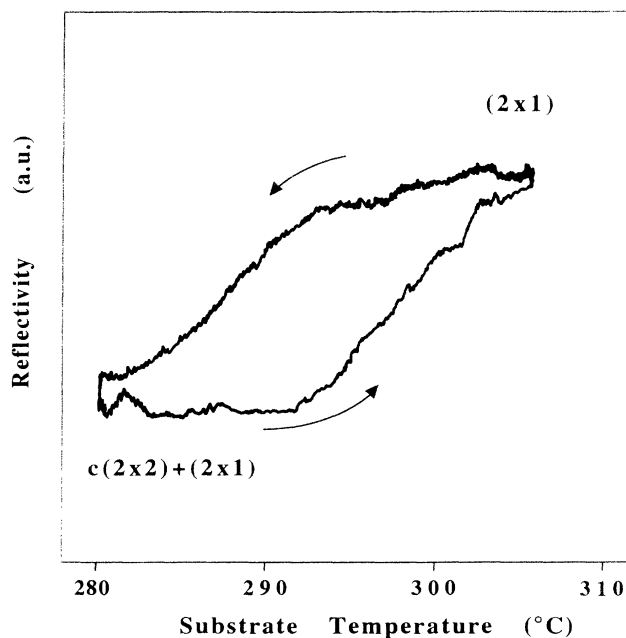


FIG. 5. Variation of the RHEED reflectivity intensity as a function of the substrate temperature for (001) CdTe, showing the reversible transformation between the $c(2 \times 2) + (2 \times 1)$ and the (2×1) surface reconstruction under vacuum. The temperature variation rate is 2 °C/min.

(2×1) surface is formed by exposing the CdTe surface to a Te flux at 310 °C. Then the Te flux is shuttered until a plateau is obtained in the RHEED specular-beam intensity [see Fig. 1(c)]. The surface reconstruction is still (2×1) . The temperature is then decreased at a rate of 2 °C/mn. Between 310 and 293 °C a sharper decrease of the intensity is observed, and simultaneously a half-order reconstruction appears in the (100) direction, showing that $c(2 \times 2)$ domains have formed. The intensity of this half-order streak increases with time. On reaching 280 °C, the sample is reheated with the same rate: no change is observed in the specular-beam intensity until 293 °C (Fig. 5). Above this temperature, the intensity increases and the $c(2 \times 2)$ surface disappears progressively, leading to the formation of an essentially (2×1) reconstructed surface.

The results obtained for the Te and Cd desorptions could partially explain the reversible transformation described above. First, we recall our observation that both the Cd and the Te desorptions lead to a (2×1) stabilized surface above 300 °C while a $c(2 \times 2) + (2 \times 1)$ reconstruction is present between 285 and 300 °C, whatever the starting surface. Then in the reversible transformation cycle, a sample heated above 300 °C should exhibit a (2×1) surface while cooling between 290 and 300 °C should lead to the reappearance of $c(2 \times 2)$ domains.

It is also interesting that temperatures higher than 293 °C correspond to the layer-by-layer sublimation regime (see Fig. 3). Consistent with the results on Cd and Te desorptions, it is therefore expected that the Cd atom desorption is stopped below this temperature when cool-

ing the sample down, while the Te surface atom desorption still occurs below 293°C. Hence, the coexistence of differently reconstructed domains could be associated with (2×1) islands "frozen" during cooling while the remaining surface still evolves to a $c(2 \times 2)$ reconstruction through Te desorption. (In any case, it is not yet clear why the relative proportions of each domain are equal.) A complete understanding of the atom mechanisms involved in the reversible transformation would require a detailed knowledge of the surface reconstructions, which is not yet available.

To sum up Sec. III, it appears that there is a unique desorption activation energy of 1.96 ± 0.05 eV for Cd, whereas a value of 0.96 ± 0.10 eV (and also about 0.7 eV in the 285–300°C range) was found for Te indicating that this species is much less strongly bonded to the (001) surface than Cd is. As a consequence, heating a Te-rich surface results in Cd enrichment of the (001) surface up to 293°C, then Cd starts to desorb, causing the materials sublimation. Further cooling the refreshed surface below 293°C allows us to restore the Cd-rich phase reversibly, due to Te desorption.

IV. (111)B CdTe

For the Te-terminated (111)B orientation, Te and Cd, desorption were studied in the 235–260°C and in the 275–305°C temperature range, respectively.

A. Te desorption

On exposing the (111)B surface to a Te flux, a (1×1) surface reconstruction is observed in the 235–260°C temperature range. After cutting off the Te flux, evolution towards a $(2\sqrt{3} \times 2\sqrt{3})R30^\circ$ surface reconstruction is observed. Figure 6(a) shows the variation of the specular-

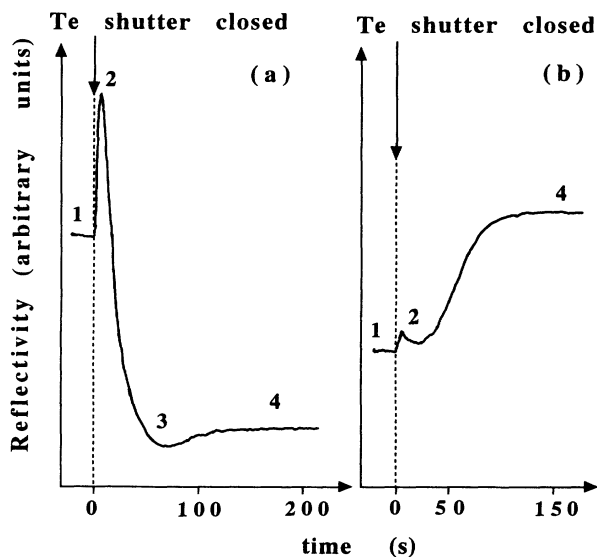


FIG. 6. (a) Change of the RHEED specular-beam reflectivity as a function of time after shuttering of the Te flux for (111)B CdTe, at $T_s=238^\circ\text{C}$. Four stages are identified, marked 1, 2, 3, and 4. (b) Change of the half-order reconstruction intensity in the same conditions as in (a). Note that the stage 3 is not clearly seen.

beam intensity. Two intermediate steps are observed before the stabilization of the final surface. We designate by 1, 2, 3, and 4 the initial, intermediate, and final steps, respectively. It was found that all the transitions from one step to the next are thermally activated. Figure 6(b) shows the change of the half-order reconstruction intensity in the $[1\bar{1}0]$ azimuth after stopping the Te flux. Consistent with Fig. 6(a) (step 2), we note an increase of the signal at very short time followed by a slow evolution towards the final step. Step 3 is not observed clearly in Fig. 6(b), indicating a low sensitivity of the intensity of the half-order streaks to the corresponding phenomena. The first increase observed just after the interruption of the Te flux could be tentatively assigned to the appearance of a transitory second-order reconstruction. The latter point will be discussed hereafter.

The time for the complete change from step 1 to step 4 is plotted in Fig. 7 as a function of $1/T_s$, as observed via both the specular-beam intensity and the surface reconstruction. A unique straight line is obtained, giving an activation energy of 2.04 ± 0.10 eV.

Furthermore (see Fig. 8), the activation energy corresponding to the change from step 1 to step 2 is found to be 1.90 ± 0.10 eV. From step 2 to step 3, it is 1.96 ± 0.10 eV and from step 3 to step 4, 2.10 ± 0.10 eV. These results indicate that the same process probably governs the different steps that we tentatively assign to the various stages of the Te desorption.

The attribution of steps 2 and 3 to ordered surfaces intermediate between the (1×1) and the $(2\sqrt{3} \times 2\sqrt{3})R30^\circ$ surfaces is supported by the results of an additional experiment. The change of the specular-beam intensity has been measured as a function of temperature under exposure of the surface to a moderate Te flux (5×10^{-7} Torr). The result shown in Fig. 9 confirms the phase diagram proposed by Duszak *et al.*¹⁵ The surface reconstruction evolves from a (1×1) to a $(2\sqrt{3} \times 2\sqrt{3})R30^\circ$ type between 250 and 320°C with two intermediate steps, namely a

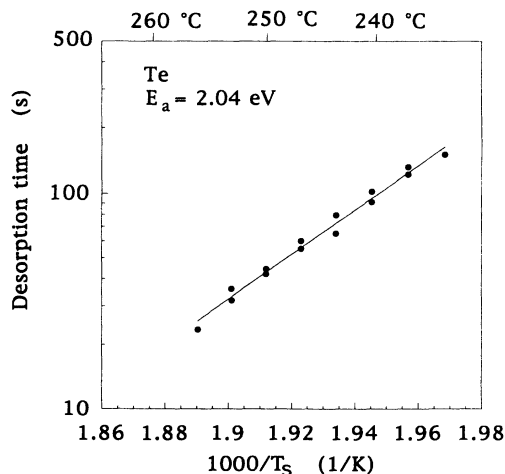


FIG. 7. Desorption time of Te from (111)B CdTe as a function of $1/T_s$ in the 230–260°C temperature range, corresponding to the full evolution from step 1 to step 4 seen in both the specular-beam intensity and the half-order reconstruction intensity.

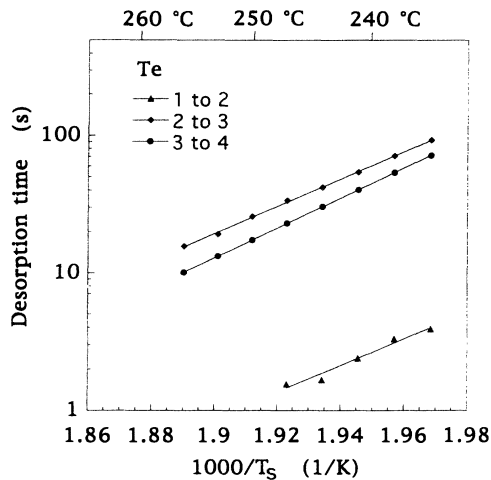


FIG. 8. Desorption time of Te from (111)*B* CdTe as a function of $1/T_s$ in the 230–260°C temperature range, corresponding to the evolution from step 1 to step 2, from step 2 to step 3, and from step 3 to step 4, as defined in Fig. 6(a). The activation energies are 1.91, 1.96, and 2.16 eV, respectively.

(2×2) and a $c(8\times 4)$ reconstruction. The change in the reconstruction type induces a change in the RHEED intensity level. Interestingly, the temperature range of stability of the (2×2) reconstruction is very narrow, suggesting that this surface is very unstable and could correspond to step 2 of the Te desorption process, which is also very sharp, as seen in Fig. 6(a). This interpretation is further reinforced by the observation of an increase of the half-order reconstruction on a time scale corresponding to step 2 in Fig. 6(b). Provided the above assumption is correct, step 3 should, therefore, be attributed to the formation of the $c(8\times 4)$ surface, which is also transitory between the (1×1) and the $(2\sqrt{3}\times 2\sqrt{3})R 30^\circ$ reconstructions. Note that the differences in the relative values of the specular-beam intensity for the Te desorption experiment and for heating under a Te pressure is due to the observation along two different azimuths, namely $[1\bar{1}0]$

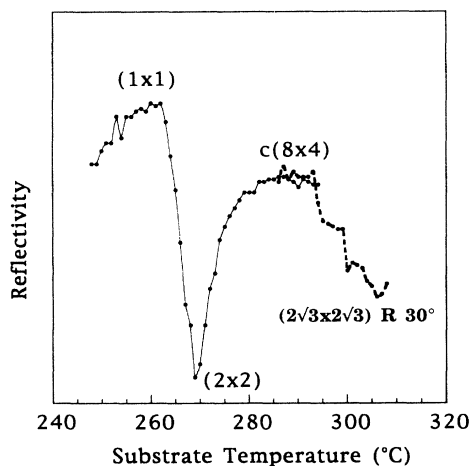


FIG. 9. Change in the RHEED reflectivity as a function of temperature for (111)*B* CdTe, along the $[1\bar{1}\bar{2}]$ azimuth, in presence of a weak Te flux ($P = 2 \times 10^{-7}$ torr). The temperature was stabilized for each point.

and $[1\bar{1}\bar{2}]$, respectively.

We attribute the measured activation energies for each step of the desorption process to the desorption of Te atoms bound to three Cd leading to the succession of different surface reconstructions with different Te coverages in the external layer, as proposed for example by Duszak *et al.*¹⁵ The percentage of Te atoms desorbed in the step 1 to step 2 transition can be tentatively deduced by observing the results obtained by Fashinger, Sitter, and Juza in atomic layer epitaxy (ALE).¹⁶ In their experiments, the surface is successively exposed to a Te and a Cd flux, with a dead time of 0.2 s between successive exposures. Plotting the epitaxial growth rate of CdTe as a function of substrate temperature, these authors observe a plateau corresponding to 1 ML/cycle below 280°C but of about 0.8 ML/cycle in the substrate temperature range 280–300°C. In the latter range, extrapolation of the data reported in Fig. 8 reveals that the time corresponding to the step 1 to step 2 process is very short (below 0.2 s) and so the decrease of the growth rate observed in ALE could result from the desorption of Te atoms during this process. Thus, the fractional coverage of Te atoms desorbed during the step 1 to step 2 transition can be tentatively estimated as 20%. Nevertheless, models of the surface structure would be necessary for a complete understanding of the phenomena.

The presence of an unstable state during evolution from step 1 to step 3 is attributed to the formation of the transitory (2×2) surface. Hence, assuming that step 3 corresponds to the formation of the $c(8\times 4)$ surface, one would expect to observe a first-order transition with hysteresis during evolution from the (1×1) to the $c(8\times 4)$ surfaces. Such a behavior has been observed in the case of InAs (001) (Refs. 17 and 18) for the transition from As-stable (2×4) to In-stable (4×2) reconstruction. The hysteresis experimentally observed in that study was related to the existence of a metastable state correlated to the slowing of As desorption in the neighborhood of the transition. As a matter of fact, as is shown in Fig. 10, such an hysteresis is observed in the case of (111)*B* CdTe

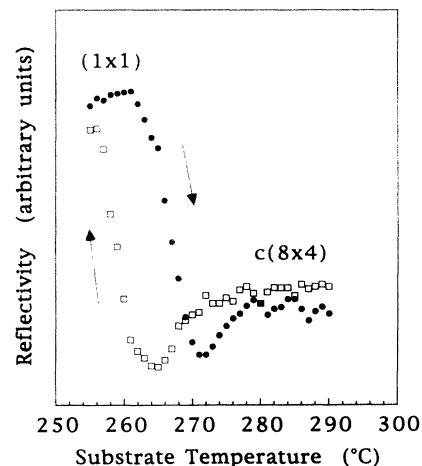


FIG. 10. Hysteresis observed when cycling the (111)*B* CdTe surface between 250 and 290°C in presence of a Te flux corresponding to a pressure of 5×10^{-7} torr. The rate of temperature variation is 1°C/min.

when recording the specular-beam intensity as a function of increasing and decreasing temperature, in the 250–280 °C temperature range and under Te pressure.

The temperature width of the hysteresis cycle is about 10 °C and does not depend on the temperature variation rate. By contrast, the dip associated with the (2×2) reconstruction was found to depend strongly on the temperature rate as was expected for a reconstructed state, with a narrow temperature range of stability. The intermediate surface is still visible in Fig. 10 for rate of temperature variation of 1 °C/mn, while for a 2 °C/mn rate it was completely smoothed, which confirms the instability of that (2×2) reconstructed surface. The hysteresis could, therefore, be related to the existence of the metastable (2×2) surface, which slows the rate of Te desorption during the first-order transition.

B. Cd desorption

Cadmium desorption was studied in the 275–305 °C temperature range. In agreement with Wu *et al.*,¹² no significant desorption could be detected in times of order several minutes at temperatures below 275 °C. Figure 11 shows the variation of the RHEED signal after interrupting the Cd flux. The surface was initially (1×1) reconstructed and evolved to a $(2\sqrt{3}\times 2\sqrt{3})R 30^\circ$ reconstruction after stopping the Cd flux. Clearly, two different behaviors are observed at low and high temperatures. A slow evolution towards equilibrium is observed

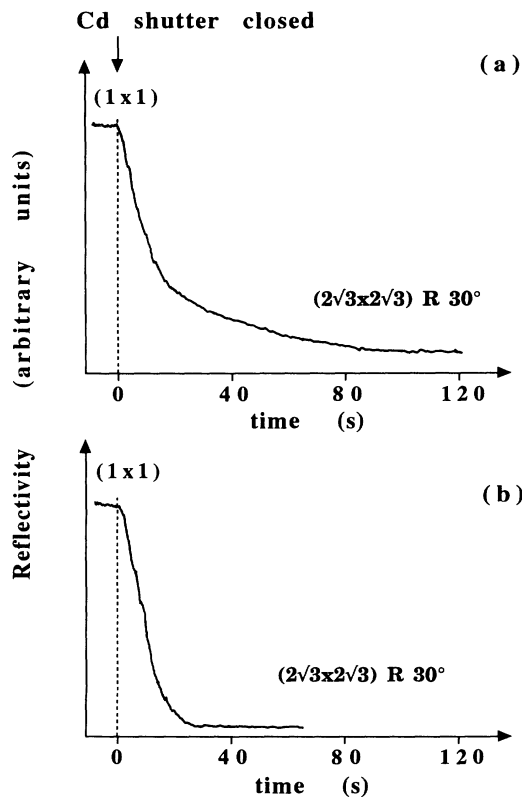


FIG. 11. Change of the RHEED intensity as a function of time when shuttering the Cd flux for (111)B CdTe. (a) $T_s = 290^\circ\text{C}$, (b) $T_s = 293^\circ\text{C}$.

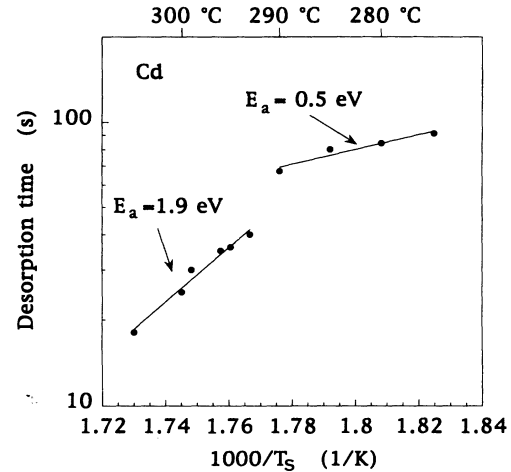


FIG. 12. Desorption time of Cd from (111)B CdTe as a function of $1/T_s$ in the 270–310 °C temperature range, showing the presence of two regimes.

at low temperature. But above 290 °C, the time necessary for reaching equilibrium is very much shorter, suggesting a drastic change in the desorption kinetics. This behavior is unambiguously shown in Fig. 12, where the desorption time was plotted as a function of $1/T_s$. Two activation energies are found: 1.9 ± 0.1 eV above 290 °C and 0.5 ± 0.1 eV below 290 °C. The discontinuity in the data for T_s in the 290–293 °C temperature range suggests a dramatic change in the Cd desorption regimes. A detailed analysis of the desorption time was made by plotting, as a function of time, the RHEED reflectivity normalized to its value under Cd saturation. The result, shown in Fig. 13, demonstrates that two desorption regimes are present below 295 °C, whereas a unique regime governs the Cd desorption above that temperature. Moreover, the fast desorption regime appears to be unique in the whole temperature range, with an activa-

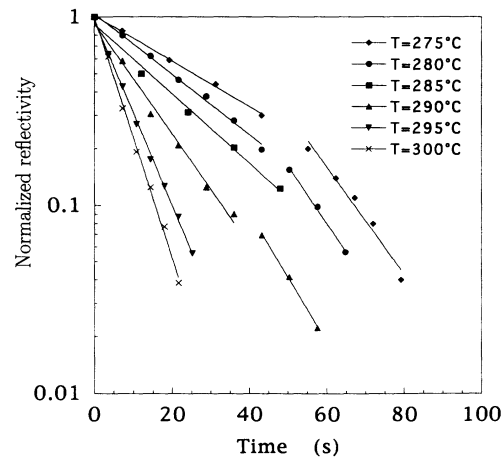


FIG. 13. Change in the RHEED reflectivity of (111)B CdTe as a function of time, normalized to its value just before Cd shuttering, for various temperatures. Two regimes are shown below 295 °C. The activation energy of the short-time regime is 1.9 eV.

tion energy of 1.9 eV.

To summarize Sec. IV, an activation energy of about 2.04 eV is found for Te desorption, with different steps in the desorption process corresponding to different intermediate surface reconstructions. These surfaces are tentatively identified as the successive surfaces observed when a sample exposed to a Te flux is progressively heated, the activation energy of 2.04 ± 0.10 eV being attributed to the desorption energy of triply bound Te atoms. For Cd, approximately the same activation energy is found above 290°C (1.9 ± 0.1 eV), while a smaller energy (about 0.5 eV) is measured below this temperature. The comparison between Te and Cd desorption shows, in agreement with XPS results,¹² that Te desorption occurs at a significantly lower temperature than Cd desorption. The two processes have about the same activation energy (2.04 and 1.9 eV) but very different preexponential factors. It is worth noting that the activation energy calculated for Cd desorption and Te desorption is about the same as the activation energy measured for the sublimation of (111)*B* CdTe, which occurs, as for the (001) orientation, in a layer-by-layer mode.^{2,11}

Recently,¹⁰ we have proposed that the layer-by-layer sublimation process of the two CdTe surfaces (001) and (111)*B* can be described by a two-step mechanism, namely a fast regime and a slow regime. The fast regime corresponds to the rapid desorption of surface atoms not involved in the reconstruction stage observed during the sublimation process. In the temperature range explored (300–400°C), the sublimation kinetics are governed for both surfaces by a common process (the slow regime), leading to a unique activation energy value of 1.90 eV. The fact that the behavior observed for Cd desorption from the (111)*B* surface above 293°C is very similar to that observed for Cd desorbing from the (001) CdTe surface, with almost the same desorption activation energy (1.9 compared to 1.96 eV), could indicate that the sublimation process is essentially governed by the desorption of Cd atoms bound in a similar way on the two surfaces. Such an interpretation would be in agreement with the models proposed for (001) and (111)*B* CdTe surfaces,^{11,15} which invoke the existence of Cd bound to two Te atoms in both cases. However, the activation energy measured for Te on (111)*B* surfaces (2.04 eV) indicates that the desorption of triply bound Te atoms could also govern the sublimation mechanism.

In fact it is difficult to discriminate between these two possibilities given that the models proposed for the $c(2 \times 2)$ Cd stabilized (001) surface and for the (2×2) , $c(8 \times 4)$, and $(2\sqrt{3} \times 2\sqrt{3})R30^\circ$ (111)*B* surfaces^{8,11} suggest that the upper layers are constituted of both Cd atoms bound to two Te and of Te atoms bound to three Cd. The desorption of a Cd or a Te therefore implies a decrease in the number of bonds of the Te or Cd atoms bound to the desorbed atom, which results in their fast desorption. The latter remark could explain that the same energies (about 1.9 eV) are found for Cd and Te desorption from the (111)*B* surface, for Cd desorption from (001) surface, and for the sublimation of both (001) and (111)*B* surfaces. The lower value found for Te on (001) surface likely refers to Te atoms bound to only two

or one Cd. A precise model of the (2×1) Te stabilized surface would be necessary to elucidate the latter point.

V. (110) CdTe

The experiments on (110) CdTe were performed in the 225–260°C temperature range. As was observed for (111)*A* CdTe,⁵ no measurements of Cd desorption could be done, that is no RHEED intensity change was observed on exposing the surface to a Cd flux. Following the conclusions of Sec. IV this could be explained by the high activation energy expected for the desorption of triply bonded Cd atoms present on these surfaces.

The change in RHEED specular-beam intensity on interruption of a Te flux is shown in Fig. 14. Clearly two steps are present. The first one (at low temperature), corresponds to an increase of the specular-beam intensity. This step is thermally activated but no precise activation energy could be measured, due to the very short time scale of the phenomenon and to the narrow range of observation temperature. The second step, observed in the whole temperature range, leads to the final surface. The decay time corresponding to the final step is plotted in Fig. 15 as a function of $1/T_s$. The activation energy is 1.23 ± 0.10 eV. Note that no measurements could be performed above 260°C, due to the surface degradation, which ultimately resulted in faceting. It is worth pointing out that an energy of 1.4 eV is obtained for Te desorption from (111)*A* CdTe.⁵ This value is not far from the value obtained in the present study for Te desorption from the (110) surface. Although this could be fortui-

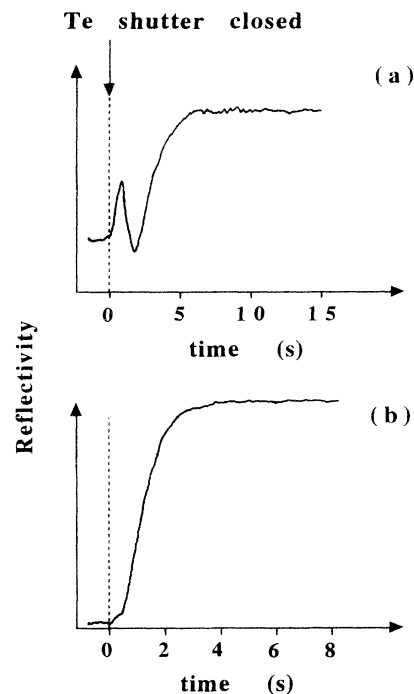


FIG. 14. Change in the RHEED reflectivity as a function of time after interruption of Te flux for (110) CdTe. (a) $T_s = 236^\circ\text{C}$, (b) $T_s = 245^\circ\text{C}$.

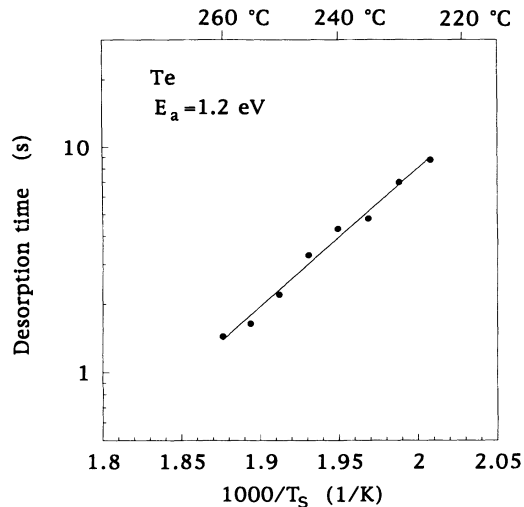


FIG. 15. Desorption time of Te from (110) CdTe as a function of $1/T_s$ in the 225–260°C temperature range.

tous, we think rather that it is related to the crystallographic structure of the (110) CdTe surface, which can be viewed as a mixture of (111)B and (111)A surfaces.

VI. CONCLUSION

The activation energies for desorption of Cd and Te have been determined for (001), (111)B, and (110) oriented CdTe surfaces. With the noticeable exception of Cd desorbed from (111)B below 290°C, which has an activation energy of 0.5 ± 0.1 eV, approximately the same Cd desorption activation energy was found for both the (001) and (111)B CdTe surfaces, namely 1.96 ± 0.10 and 1.9 ± 0.1 eV, respectively, which could be due to equivalent bonding configurations, that is a Cd bound to two Te. As concerns Te, the situation is far more complex because desorption activation energies of 0.96, 1.23, and 2.04 ± 0.10 eV are found for (001), (110), and (111)B CdTe surfaces, respectively. The activation energy of 2.04 eV found for (111)B CdTe is attributed to the

desorption of triply bound Te atoms. The fact that the same activation energy is obtained for Cd desorption from (001) and (111)B CdTe and for Te desorption from the (111)B surface can be interpreted as follows. It probably represents the interdependence of the desorption of twofold bound Cd atoms and of threefold bound Te atoms, due to their simultaneous presence in the surface reconstructions obtained in Cd-rich conditions on (001) CdTe and in Te-rich conditions on (111)B CdTe. Our conclusion is, therefore, that the activation energy value 1.9 eV is characteristic of the sublimation regime and of the interdependent desorption of Cd and Te. This is consistent with the reverse RHEED oscillations experiments from which a sublimation activation energy of 1.9 eV was found for both (001) and (111)B CdTe. An additional conclusion is that sublimation occurs above about 290°C for both surfaces, consistent with ALE experiments^{16,19} demonstrating that a growth rate smaller than 1 ML/cycle is obtained for both (001) and (111)B CdTe above 290°C.

We have also shown in the present study that, starting from (111)B and (110) CdTe surfaces stabilized under Te pressure, the evolution towards the under vacuum-stabilized surface occurs through different intermediate surfaces. In particular, the presence of a transitory surface on (111)B CdTe, which is stable in a very narrow temperature range, was found to be responsible for the hysteresis phenomenon seen on the (111)B surface during temperature cycles under a Te flux.

On (001) CdTe the existence of a reversible transformation under vacuum has been confirmed and was partially explained by the existence of different desorption rates for Cd and Te.

The Cd and Te desorption experiments reported above provide useful enlightenment on the choice of CdTe growth conditions in molecular-beam epitaxy. In particular, the empirical observation that a better smoothing of the (001) surface is achieved with Te than with Cd is consistent with the activation energy found for Te desorption from that surface, suggesting that the surface roughening mainly occurs through Te loss. Similarly, a Te excess is necessary for the growth of (111)B CdTe in the temperature range 300–330°C, as well as for (110) CdTe growth in the whole temperature range.

¹J. D. Benson, B. K. Wagner, A. Torabi, and C. J. Summers, *Appl. Phys. Lett.* **49**, 1034 (1986).

²J. M. Arias and G. Sullivan, *J. Vac. Sci. Technol. A* **5**, 3143 (1987).

³P. Juza, W. Faschinger, K. Hingerl, and H. Sitter, *Semicond. Sci. Technol.* **5**, 191 (1990).

⁴A. Waag, T. Behr, T. Litz, B. Kuhn-Heinrich, D. Hommel, and G. Landwehr, *Mater. Sci. Eng. B* **16**, 103 (1993).

⁵Y. S. Wu, C. R. Becker, A. Waag, K. Von Schierstedt, R. N. Bicknell-Tassius, and G. Landwehr, *Appl. Phys. Lett.* **62**, 1510 (1993).

⁶H. Yamaguchi and Y. Horikoshi, *J. Appl. Phys.* **71**, 1753

(1992).

⁷C. Deparis and J. Massies, *J. Cryst. Growth* **108**, 157 (1991).

⁸R. Duszak, S. Tatarenko, J. Cibert, K. Saminadayar, C. Deshayes, *J. Vac. Sci. Technol. A* **9**, 3025 (1991).

⁹S. Tatarenko, F. Bassani, J. C. Klein, K. Saminadayar, J. Cibert, and V. H. Etgens, *J. Vac. Sci. Technol. A* **12**, 140 (1994).

¹⁰S. Tatarenko, B. Daudin, and D. Brun, *Appl. Phys. Lett.* **65**, 734 (1994).

¹¹V. H. Etgens, S. Tatarenko, J. C. Klein, M. B. Veron, J. Cibert, K. Saminadayar, M. Sauvage-Simkin, and R. Pinchaux, *The Fourth International Conference on the Formation of Semiconductor Interfaces, Julich, 1993* (World Scientific,

- Singapore, 1994), p. 67.
- ¹²Y. S. Wu, C. R. Becker, A. Waag, M. M. Kraus, R. N. Bicknell-Tassius, and G. Landwehr, *Phys. Rev. B* **44**, 8904 (1991).
- ¹³W. Chen, A. Kahn, P. Soukassian, P. S. Mangat, J. Gaines, C. Ponzoni, and D. Olego, *Phys. Rev. B* **49**, 10 790 (1994).
- ¹⁴P. John, F. M. Leibsle, T. Miller, T. C. Hsieh, and T. C. Chiang, *Superlatt. Microstruct.* **3**, 347 (1987).
- ¹⁵R. Duszak, S. Tatarenko, J. Cibert, N. Magnea, H. Mariette, and K. Saminadayar, *Surf. Sci.* **251/252**, 511 (1991).
- ¹⁶W. Fashinger, H. Sitter, and P. Juza, *Appl. Phys. Lett.* **53**, 2519 (1988).
- ¹⁷J. M. Moison, C. Guille, and M. Bensoussan, *Phys. Rev. Lett.* **58**, 2555 (1987).
- ¹⁸H. Yamaguchi and Y. Horikoshi, *Phys. Rev. B* **45**, 1511 (1992).
- ¹⁹W. Fashinger and H. Sitter, *J. Cryst. Growth* **99**, 566 (1990).